

# Error Analysis of a Low–Low Satellite-to-Satellite Tracking Mission

Jeongrae Kim\* and Byron D. Tapley†  
*University of Texas at Austin, Austin, Texas 78759*

**The Gravity Recovery and Climate Experiment is a dedicated spaceborne mission whose objective is to map the gravity field with unprecedented accuracy. It consists of two satellites coorbiting in a nearly polar orbit at low altitude. Primary measurements are a series of measured range changes between the two satellites using a dual one-way microwave ranging system. These measurements are combined with accelerometer and global positioning system measurements. In this study, comprehensive simulation models for these major instruments have been developed to recover the gravity information. Effects of the primary error sources on the orbit and gravity estimation are analyzed through a series of numerical simulations.**

## I. Introduction

**T**HE accurate determination of the Earth's gravity field is essential for a wide variety of geophysical applications, including oceanography, hydrology, glaciology, geodesy, and solid Earth science.<sup>1</sup> The Gravity Recovery and Climate Experiment (GRACE), selected under the NASA Earth System Science Pathfinder program, is a dedicated spaceborne mission whose objective is to map the gravity field with unprecedented accuracy. The mission involves two satellites orbiting in the same plane in a low–low satellite-to-satellite tracking (SST) mode. The two satellites were launched in March 2002 with a five-year mission lifetime.<sup>2</sup>

The orbit of any satellite in a near Earth orbit is dependent on the globally integrated effect of the mass distributions and movements in the Earth system. The orbits of two satellites, sensing these effects at slightly different phases, are perturbed differentially.<sup>3</sup> This difference in perturbations is manifested in the intersatellite range change. With this concept, the GRACE mission consists of two coorbiting satellites at 300–500 km altitude with a  $220 \pm 50$ -km along-track separation. The GRACE microwave ranging instrument can provide very accurate measurements of the range changes. When these differential measurements are made, the higher-frequency content of the gravitational signals is amplified, thus enabling significant improvement in the estimates of the higher resolution features of the Earth's gravity field. Because the separation distance is small, the errors due to media effects are minimized as compared to space-based or ground-based tracking. The orbit inclination is close to 90 deg to maximize global coverage.

The satellite orbits and their relative positions are affected not only by the gravitational accelerations, but also by nongravitational accelerations, and their effects must be accurately measured to utilize the gravitational information in the range change measurements. For this purpose, each GRACE satellite carries a high-precision three-axis accelerometer (ACC). Each satellite also carries a geodetic-quality global positioning system (GPS) receiver to ensure that the orbits for the satellites can be continuously and accurately determined and that the gravity field estimates can be correctly registered in a terrestrial reference frame. The overall dimension of each

GRACE satellite<sup>4</sup> is approximately  $3.1 \times 1.9 \times 0.7$  m (length times width times height) with an initial mass of 425 kg.

The mission is implemented as a joint project between NASA and the German Aerospace Research Establishment, DLR. The mission is implemented under the overall direction of the University of Texas/Center for Space Research (UT/CSR). NASA Jet Propulsion Laboratory, California Institute of Technology (JPL) has been assigned responsibility for the development of the science instrument and satellite system in partnership with Space Systems/Loral and Dornier Satellitensysteme. The DLR German Space Operation Center (GSOC), with its ground-tracking facilities, is responsible for the operation of the GRACE satellites. The observation data collected by GSOC are processed in a cooperative approach by UT/CSR, JPL, and GeoForschungsZentrum in Germany.

The advantage of using a pair of coorbiting satellites for gravity detection was first described by Wolff.<sup>5</sup> The equations of motion for a near-Earth satellite in orbit contain the gravitational potential; its variations affect the motion of the satellite. This is easily envisioned through the observation of energy. If the gravitational energy should change, it must be accounted for by a change of the kinetic energy terms, where the time-dependent potentials such as the sun's are ignored. When two coorbiting satellites' total energies are subtracted, the velocity difference of the two satellites becomes directly proportional to the geopotential difference at their respective locations. This is the basic concept, but it neglects the effects of time-varying, nonconservative surface forces.

Based on this low–low SST concept, the NASA Gravity Research Mission (GRM) was proposed in 1980s, but was never implemented. It was similar to the GRACE mission except for the use of a drag compensation system instead of the ACC and the lack of the GPS receiver.<sup>5–7</sup> There have been many studies on the GRM and general SST missions.<sup>8–11</sup>

Most of the previous studies utilized analytic or semi-analytic methods to evaluate the gravity estimation accuracy from the SST mission. Direct mapping of the relative velocity or the range-rate observations to the gravity field was usually used for predicting the estimated gravity accuracy. These analytic approaches were limited by simplified models and certain assumptions.

A more general and comprehensive approach is based on a full numerical simulation. Instead of using the mapping functions, each satellite's orbit is estimated, along with the gravity field, by using a least-squares batch estimation algorithm.<sup>12,13</sup> This approach enables implementation of more comprehensive instrument models and relaxes certain limitations, for example, the orbits must be in repeating ground tracks.

The principal objective of this study was to provide the information for the satellite design and orbit selections through a comprehensive simulation analysis. A high-fidelity numerical simulation approach was used, with an emphasis on comprehensive instrument error modeling, to obtain realistic simulation results.

Received 13 April 2001; revision received 22 May 2002; accepted for publication 11 July 2002. Copyright © 2002 by Jeongrae Kim and Byron D. Tapley. Published by the American Institute of Aeronautics and Astronautics, Inc., with permission. Copies of this paper may be made for personal or internal use, on condition that the copier pay the \$10.00 per-copy fee to the Copyright Clearance Center, Inc., 222 Rosewood Drive, Danvers, MA 01923; include the code 0731-5090/02 \$10.00 in correspondence with the CCC.

\*Research Associate, Center for Space Research; currently Rocket System Department, Korea Aerospace Research Institute, Daejeon 305-333, Republic of Korea; jrkim@csr.utexas.edu. Senior Member AIAA.

†The Clare Cockrell Williams Chair and Director, Center for Space Research; tapley@csr.utexas.edu. Fellow AIAA.

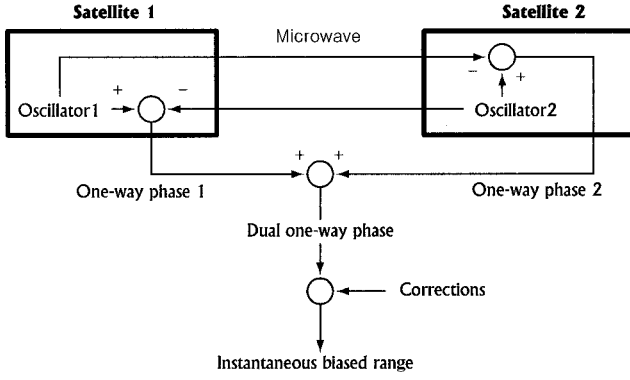


Fig. 1 Dual one-way ranging system.

## II. Measurement Models

This section describes two major instrument models, SST and ACC, with their major error sources. These models were used for a measurement simulation.

### A. SST Model

A biased range between the GRACE satellites is the primary measurement for the GRACE mission. The dual one-way ranging system provides micrometer-level accuracy for this type of measurement. The most dominant error source for the microwave ranging measurement is the instability of the oscillator that drives the microwave signal. The dual one-way ranging system minimizes the oscillator instability by combining two intersatellite ranging measurements.

Figure 1 shows a concept for the dual one-way ranging system. With identical transmission and reception subsystems, each satellite transmits a carrier phase signal to the other satellite.<sup>6,7,13,14</sup> The received signal at each of the two satellites is recorded and later transmitted to the ground station. This signal is called the one-way phase measurement, and there are two one-way phases from the pair of satellites. This one-way phase is conceptually identical to the GPS phase measurement, that is, the difference between the receiver's reference phase and received phase.<sup>15</sup>

The frequency fluctuations due to oscillator instability have nearly equal and opposite effects on each one-way phase measurement. Summation of these two phases cancels the long and medium period parts of the oscillator noise. Only the high-frequency noise, whose period is shorter than the signal time of flight ( $\sim 1$  ms), remains after this process.<sup>7</sup> This concept is similar to the single difference in the GPS measurement processing.<sup>15</sup>

The combined phase measurement is called the dual one-way phase measurement. This can be converted to a range measurement by multiplication of the wavelength to obtain the following expression:

$$R(t) = \rho(t) + \Delta\rho_{\text{TOF}} + I + d + B + \Delta\rho_{\text{err}} \quad (1)$$

The dual one-way range  $R(t)$  in Eq. (1) is a sum of the instantaneous range  $\rho(t)$  and other components. The instantaneous range is the range between two satellites' c.m. at a certain instance  $t$ . The light-time correction  $\Delta\rho_{\text{TOF}}$  accounts for the satellite motion during the signal time of flight.<sup>15</sup> The phase center offset  $d$  is the distance between the antenna phase center and the satellite c.m. The range bias  $B$  results from unknown phase ambiguity values in the one-way phases. The ionosphere delay  $I$  can be estimated by using the differential time of flight in the two frequency signals'  $K$  (24 GHz) and  $Ka$  (32 GHz) bands.<sup>2,14</sup> The measurement error is represented as  $\Delta\rho_{\text{err}}$ .

During the ground preprocessing, a range correction, which is the sum of the light-time, ionosphere delay, and phase-center offset corrections, is estimated and applied to the dual one-way range  $R(t)$  to yield a biased range  $\rho_b(t)$ :

$$\rho_b(t) = R(t) - \Delta\rho_{\text{cor}} \quad (2)$$

where

$$\Delta\rho_{\text{cor}} = \Delta\rho_{\text{TOF}} + I + d \quad (3)$$

This observable represents the instantaneous range at a certain epoch with a bias and measurement errors.

Derived quantities, range rate and range acceleration, can be obtained by numerical differentiation of the series of range measurements. Either the measured biased range or derived range rate can be used for the gravity and orbit estimation process. Details on the dual one-way ranging system and its simulation procedure can be found in several references.<sup>13,14,16</sup>

The range measurement error  $\Delta\rho_{\text{err}}$  can be modeled as the summation of the following errors:

$$\Delta\rho_{\text{err}} = \Delta\rho_{\text{osc}} + \Delta\rho_{\text{time}} + \Delta\rho_{\text{sys}} + \Delta\rho_{\text{mp}} + \Delta\rho_{\text{other}} \quad (4)$$

The oscillator noise residual after the dual one-way ranging is called the SST oscillator noise in this study, identified as  $\Delta\rho_{\text{osc}}$ . Its error level depends on the oscillator characteristics and the noise cancellation efficiency of the dual one-way ranging system. The time-tag related error  $\Delta\rho_{\text{time}}$  is due to the measurement time-tag error, especially the relative time-tag error between the two satellites. This is not the onboard time-tag error due to the oscillator instability, but the ground processed time-tag error after corrections are applied with the aid of the GPS measurements. The raw one-way phase measurements are interpolated to the corrected time tag on the ground; the effect of the time-tag error becomes much smaller after this process. Another error source is the system noise  $\Delta\rho_{\text{sys}}$  due to the receiver instrument noise. The multipath error  $\Delta\rho_{\text{mp}}$  is due to indirect signals that arise when the line of sight of the two satellites is not perfectly aligned with the microwave antenna boresight. The other error,  $\Delta\rho_{\text{other}}$ , represents negligible error sources whose error levels were tested in separate simulations and not included in this study.

In summary, the output from each satellite is the one-way phase, and it is sent to the ground. The output from the dual one-way ranging system is the biased range between two satellites' c.m. after ground preprocessing.

### B. ACC Model

Each GRACE satellite carries an electrostatic three-axis ACC that measures the electrostatic force necessary to maintain the ACC proof mass motionless with respect to the sensor cage. The proof mass should be located at the mass center of each satellite.

The ACC measurement is the sum of the nongravitational accelerations, including atmospheric drag, radiation pressure, and thrust, but this measurement is corrupted by various error sources. The following formulation describes the measurement models for simulation of the ACC measurement.

The ACC measurement model is given by<sup>13,17</sup>

$$\mathbf{f}^{\text{obs}} = \mathbf{M}(\mathbf{R}_{S \rightarrow \text{ACC}}^{\text{err}} \mathbf{R}_{I \rightarrow S}^{\text{true}} \mathbf{f}^I) + \mathbf{b} + \mathbf{S} + \mathbf{f}_{\text{c.m.}} + \mathbf{f}_{\text{other}} \quad (5)$$

where  $\mathbf{f}^I$  represents the true nongravitational acceleration expressed in inertial coordinates and  $\mathbf{f}^{\text{obs}}$  represents the observation. The rotation matrix  $\mathbf{R}_{I \rightarrow S}^{\text{true}}$  represents the coordinate transform from the inertial ( $I$ ) to the satellite body-fixed ( $S$ ) coordinates. Another rotation matrix,  $\mathbf{R}_{S \rightarrow \text{ACC}}^{\text{err}}$ , is from the satellite-body-fixed  $S$  to the ACC coordinates. Because of misalignment during the ACC installation, the satellite and ACC axes may not be coincident. This difference is assumed unknown and treated as the misalignment error. The  $(3 \times 3)$  scale factor matrix  $\mathbf{M}$  contains scale factors, and the  $(3 \times 1)$  vector  $\mathbf{b}$  contains biases. The instrument random noise is represented as  $\mathbf{S}$ .

The c.m. offset-induced error  $\mathbf{f}_{\text{c.m.}}$  results from the difference between the ACC proof-mass location and the satellite c.m. The coupling between the c.m. offset and satellite attitude motion produces some parasitic accelerations. The last term,  $\mathbf{f}_{\text{other}}$ , represents other error sources that are negligible or not included in this study. These error sources will be discussed further in the simulation error model section.

Another measurement type is the attitude observation from the star trackers. This measurement provides the coordinate transformation between the inertial and satellite body-fixed coordinates:

$$\mathbf{R}_{I \rightarrow S}^{\text{obs}} = \mathbf{R}_{I \rightarrow S}^{\text{err}} \mathbf{R}_{I \rightarrow S}^{\text{true}} \quad (6)$$

The matrix  $\mathbf{R}_{I \rightarrow S}^{\text{err}}$  represents the attitude measurement error. Note that this is not the attitude control error, but the attitude knowledge

error. In summary, the measurement equations (5) and (6) have two types of errors, measurement error ( $M, b, S, f_{c.m.}, f_{err}$ ) and coordinate transformation error ( $R_{S \rightarrow ACC}^{err}, R_{I \rightarrow S}^{err}$ ).

### III. Estimation Procedure

#### A. Role of GPS Measurement

The GPS signals received by each GRACE satellite provide the information for determining the GRACE satellite orbit and the measurement time tags.<sup>2</sup> The real-time GPS solutions are used by the onboard controller for the orbit control and determination of measurement time tags. For the mission's scientific purpose (gravity estimation), more refined measurements are obtained through ground processing, for example, the time-tag and ionosphere corrections. In this simulation study, only the ground-processed measurements were considered for the orbit information.

The estimation of the GRACE satellite orbits by using only the low-low SST measurements has a singularity problem due to the nature of the measurement, that is, the relative distance between the two satellites is not adequate to determine the absolute position of each. The orbit information from the GPS measurements alleviates this singularity. Because the orbit estimation is tightly coupled with the gravity estimation, the gravity information, as well as the orbit information, from the GPS measurements is necessary to obtain a well-conditioned solution.

#### B. Gravity and Orbit Estimation

A batch filter<sup>18</sup> was used for the estimation process. The estimation parameters include each satellite's initial position and velocity [initial conditions (IC)] ( $r_1 v_1 : r_2 v_2$ ), force and measurement empirical parameters for each satellite ( $Bd_i, Bm_i$ ), common empirical parameters between the two satellites ( $Bl$ ), and gravity harmonic coefficients ( $C_{nm}, S_{nm}$ ):

$$X = [r_1 v_1 : r_2 v_2 : Bd_1 Bd_2 : Bm_1 Bm_2 : Bl : C_{nm} S_{nm}]^T \quad (7)$$

Details on the empirical parameters will be discussed in the next section. Note that the orbit and gravity should be estimated simultaneously because of their high correlations. These parameters were estimated by using the SST and GPS measurements, whereas the ACC measurements replace the surface force models in the orbit integrator.

The lower part of Fig. 2 depicts the estimation procedure. The first step involves computing the nominal or preliminary orbits by use of the GPS measurements. This process forces the nominal orbits to be in the linear region of the true orbits to apply the linear estimation theory. This adjustment minimizes the solution dependency on the initial orbit errors. Other simulation experiments confirm that the

final gravity estimation accuracy is not very sensitive to the nominal orbit accuracy.

Along the nominal orbits, measurement partial derivatives with respect to the SST or GPS measurements are computed. Then each partial derivative is multiplied by an appropriate measurement weight and accumulated to form an information matrix.<sup>13</sup> These SST and GPS information matrices are combined and used to estimate the updates for the nominal parameters. New parameters are obtained by adding the updates to the nominal values.

The measurement weights, especially the relative weights between the GPS and SST information matrices, are crucial to the estimation accuracy. In the case of the simulations, it is possible to determine accurate weightings because the applied noise level is known.<sup>13</sup> Real data processing requires an iteration process to compute the optimal weightings. An optimal weighting method,<sup>19</sup> which maximizes a likelihood function, will be used for the real data processing.

#### C. Empirical Parameters

One of the ways for treating mis modeled or unmodeled measurement error is to estimate empirical measurement parameters. For the low-low SST measurements, low-low bias and drift were estimated<sup>13</sup>:

$$\begin{aligned} \rho_{obs}(t) = & \rho_{nom}(t) + C_0 + C_1 t + C_2 t^2 \\ & + (P_{C0} + P_{C1} t) \cos u + (P_{S0} + P_{S1} t) \sin u \end{aligned} \quad (8)$$

where  $\rho_{obs}(t)$  is the observation of the biased instantaneous range or range rate. The nominal or computed value is  $\rho_{nom}(t)$ , and the latitude argument of the two satellites' midpoint is denoted by  $u$ . The estimation parameters  $C_i$  and  $P_i$  are part of the common parameters  $Bl$  of Eq. (7). These bias parameters minimize the effect of the unknown measurement bias  $B$  of Eq. (1) and the low-frequency errors, especially the oscillator noise residual. For the GPS measurements, double difference biases were estimated to account for the phase ambiguities. These are classified as  $Bm_1$  and  $Bm_2$  of Eq. (7).

As with the empirical measurement parameters, empirical force parameters were estimated to treat unmodeled forces acting on the satellite. These parameters are part of the nominal force models. The nominal ACC scale factors and biases, which are used to treat the unknown scale factor and bias errors, can be classified into this category. As mentioned in Sec. II.B, the ACC measurement goes into the orbit integrator, and it is not directly used as an observation. This is why the ACC parameters are treated as force parameters instead of measurement parameters. The following equation relates the ACC observation  $f^{obs}$  with the inertial acceleration  $f^I$  used for the orbit integration:

$$f^I = R_{S \rightarrow I}^{obs} (\tilde{M} f^{obs} + \tilde{b}) \quad (9)$$

The  $(3 \times 3)$  matrix  $R_{I \rightarrow S}^{obs}$ , the transformation from the satellite body fixed to inertial coordinates, can be obtained from the attitude measurement, that is, the star camera. The nominal scale factor  $\tilde{M}$  and bias  $\tilde{b}$  are adjusted during the estimation process. These parameters are classified as  $Bd_1$  and  $Bd_2$  of Eq. (7).

### IV. Simulation Description

The simulation procedure consists of two major parts, measurement simulation and measurement processing. Two different force and measurement models, truth and nominal, are used. The truth model is used to generate the true motion and true observations. The nominal or reference model is used to start the estimation process and provides the basis for the first iteration in the estimation process. The difference between the two models represents the current uncertainty level of the force and measurement models. It also enables determination of the sensitivity of the estimation accuracy to the model errors.

Descriptions of the two models are given in Table 1 (see also Ref. 20). This section describes the simulation procedure and the orbit conditions. Then, the measurement (SST, ACC, and GPS) and force models will be described.

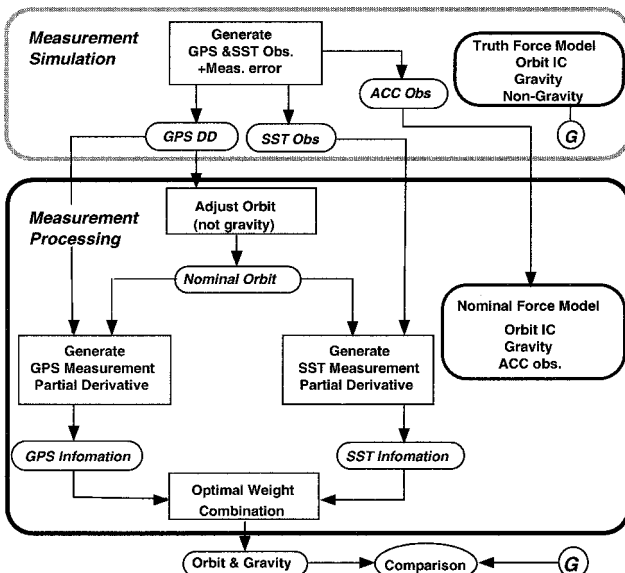


Fig. 2 Simulation procedure.

**Table 1** Simulation parameters

Type	Truth	Nominal
<i>Gravitational forces</i>		
Spherical harmonics	EGM96 (120 × 120)	EGM96 clone (120 × 120)
<i>Non-gravitational forces</i>		
Atmospheric drag	Cannon ball model	—
Density: drag temperature model <sup>20</sup>		
Solar radiation pressure	Box model	ACC
Earth radiation pressure	flux/reflectivity	measurements (including noise)
	Box model	
	albedo/emissivity	
<i>Intersatellite measurement model</i>		
System noise	1 $\mu\text{m}/\sqrt{\text{Hz}}$ at 230 km	Low-low empirical
Oscillator noise	$\approx 1/f^3$ in range	bias and bias rate
Multipath error	3 $\mu\text{m}$ per milliradian attitude variation	
<i>ACC measurement model</i>		
Bias	10 <sup>-6</sup>	Bias/scale factor
Scale factor	2%	or
Random noise	(1 + 0.005/f) × 10 <sup>-20</sup> m <sup>2</sup> /s <sup>4</sup> /Hz	constant tangential/
Alignment	0.3 mrad	1-CPR empirical
Attitude error	0.05 mrad white noise	parameters

### A. Simulation Procedure

A series of numerical simulations was performed to analyze the effect of instrument noise and orbit conditions on the gravity estimation by changing the noise and orbit conditions. From those results, one typical simulation result was selected for discussion of the expected gravity accuracy. A spherical harmonic degree and order 120 gravity field was estimated by using 32 days' worth of measurements.

Figure 2 shows a flow chart of the simulation procedure. The upper part is the measurement simulation, and the lower part is the estimation process. In the actual measurement processing, the real data replaces the upper part.

The first step of the measurement simulation is to generate simulated measurements using the truth models, that is, truth satellite IC, truth gravity field, and truth nongravitational force models. The simulated SST, GPS, and ACC measurements are obtained after applying the instrument noise. The time interval of the SST, ACC, and GPS measurements were 10, 10, and 30 s, respectively.

The estimation process was already described in the preceding section. This process estimates the difference between the truth and nominal gravity coefficients, which is used for correcting the nominal gravity coefficients. The last step is comparing the updated gravity coefficients with the truth coefficients. This difference represents the expected gravity estimation error from the GRACE mission.

The SST range-rate measurements were used with the GPS and ACC measurements. The simulation results showed that the gravity estimation using the range rate was better than the range.<sup>13</sup> These results are subject to the numerical differentiation and parameter estimation methods. The conclusion as to which data type is better for the gravity estimation should be reserved until the real data are processed.

### B. Orbit Conditions

Each satellite orbit has an 88.5-deg inclination, 448-km initial altitude, and 0.001 eccentricity. Both of the satellites are in the same orbit planes (tandem formation) and separated by 239 km. Other simulation results showed that the use of slightly different orbits (echelon formation) improved some gravity coefficients,<sup>8,11</sup> but the improvement was not significant.<sup>13</sup> Also, the echelon formation requires a higher degree of attitude control, and for this reason the tandem formation was selected for the GRACE mission. More details on the selection of the orbit conditions, for example, inclination, altitude, etc., can be found in Ref. 13.

### C. SST Error Model

For the realization of the SST range measurement errors, two approaches have been tested. One simulates the one-way phase time

series with the measurement errors. Then a time series of noisy biased range is obtained from these one-way phases and corrections.<sup>16</sup> This approach closely approximates the real data processing. The other approach simulates the range time series with the range measurement errors corresponding to the overall phase errors.<sup>13,14</sup> It uses an analytic model to map the one-way phase error to the range error. The latter approach is less computationally intensive and can be used for design studies. A comparison of these simulations demonstrates that the two approaches yield equivalent range errors. In this paper, the second approach was used for simulating either noisy range or range-rate measurements.

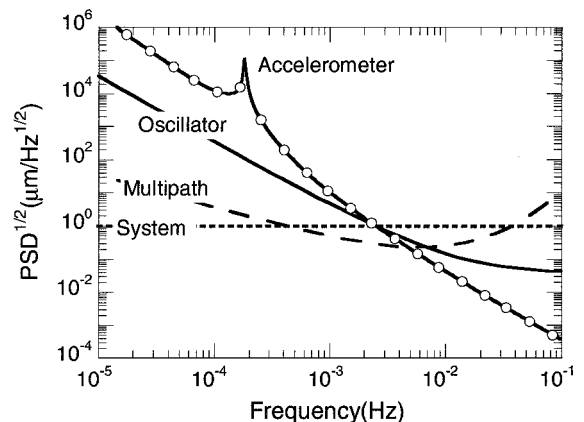
The SST oscillator noise  $\Delta\rho_{\text{osc}}$  in Eq. (4) is a function of the oscillator characteristics, frequency offset, carrier frequency, and satellite separation distance. The GRACE satellite uses a quartz crystal type ultrastable oscillator,<sup>2,14</sup> and its Allan deviations are about  $2 \times 10^{-13}$  for an averaging period of 100 s. From this specification, the phase error from the oscillator was simulated with a Gauss–Markov model (see Refs. 21 and 22) and then converted into the residual oscillator drift.<sup>13,14</sup>

The time-tag related error  $\Delta\rho_{\text{time}}$  in Eq. (4) can be ignored after resampling the phase measurements with the corrected time tags. With the GPS and International GPS Service network data, the actual measurement time tag can be estimated accurately on the ground. Other simulation experiments showed that the time-tag error effect can be ignored if the relative time-tag error between the two satellites has variability smaller than 200 ps. The bias component of the time-tag error is not a concern because it is transferred to the range bias, which can be adjusted by empirical bias parameters.

The system noise  $\Delta\rho_{\text{sys}}$  was approximated as white noise for the phase measurement.<sup>15</sup> Its magnitude varies with the distance between the two GRACE satellites or the signal-to-noise ratio. The range error power spectral density (PSD) due to this system noise was assumed as  $(1 \mu\text{m}/\sqrt{\text{Hz}})^2$  for a 230-km separation. This distance corresponds to a 2-deg separation angle at the GRACE altitude (300–500 km).

Because of the arbitrarily different geometric situations, there is no general model of the multipath error  $\Delta\rho_{\text{mp}}$ ; however, with some approximations cited in Ref. 13, it is possible to derive a simple relationship between the attitude variation and a pessimistic multipath error model. Attitude simulation results from NASA Langley Research Center/Analytic Mechanics Association, Inc., were used to obtain an attitude variation time series<sup>4,23</sup> and to realize the multipath error effects.

Figure 3 compares the PSD of the SST range errors due to the individual error sources. The range error due to the ACC random noise is also plotted for comparison. At the low frequency (less than  $2 \times 10^{-3}$  Hz), the SST oscillator noise is dominant. At the high frequencies, the SST system noise is dominant. However, all three SST errors are smaller than the ACC noise at the low frequencies. Consequently, one can predict that the accuracy of the low-degree (long-wavelength) gravity coefficients will be mainly affected by the ACC errors, whereas the high-degree (short-wavelength) gravity coefficients are mainly affected by the SST errors.

**Fig. 3** Power spectrum of intersatellite range errors.

### D. ACC Error Model

Each GRACE satellite uses a SuperSTAR ACC developed by ONERA. Its design requirement<sup>2</sup> specifies an accuracy of  $0.1 \text{ nm/s}^2$  for 10-Hz samples and a full-scale range of  $5 \times 10^{-5} \text{ m/s}^2$ . The initial (precalibrated) scale factors  $M$  and biases  $b$  are obtained during the ground (preflight) test. For the simulation studies described here, values of 2% and  $10^{-5}$  were used as errors for  $\tilde{M}$  and  $\tilde{b}$  in Eq. (9), respectively. These offsets were added to the ideal values, 1.0 (scale factor) and 0 (bias). The scale factor offsets are applied to the diagonal elements of  $M$ . This matrix  $M$  may have nonzero off-diagonal elements that reflect the cross coupling among the three axes. However, these effects on the GRACE ACC measurements are negligible, and the scale factor matrix  $M$  was assumed to have the diagonal elements only. A quadratic term ( $M' f^2$ ) is negligible as well. After the on-orbit estimation process, the uncertainty of the scale factor and bias can be reduced to 0.2% and  $10^{-6}$ . These are called postcalibrated values. After this calibration process, the effects of the scale factor and bias offsets become negligible.

The ACC random noise  $S$  was modeled to have frequency-dependent characteristics, and the design specification for its PSD was  $[(1 + 0.005/f)^{1/2} \times 10^{-10} \text{ m/s}^2/\text{Hz}^{1/2}]^2$ . Because of a ground test, one ACC axis has a lower accuracy than the other axes.<sup>14</sup> The normal (cross-track) direction was selected as the axis for this reduced sensitivity axis, which has a one order of magnitude higher noise level than the other axes. Because the cross-track motion is separated from the in-plane motion in the linear region, this reduced sensitivity has a negligible effect on the orbit and gravity estimation accuracy.<sup>13</sup>

The attitude measurement errors  $R_{f \rightarrow s}^{\text{err}}$  of Eq. (6) are mainly determined by the accuracy of two star trackers, and white noise variations were assumed for the errors in the measurements. For the misalignment error ( $R_{s \rightarrow \text{ACC}}^{\text{err}}$ ) of Eq. (5), values of 0.3 mrad were assumed and remained constant through all data spans. The time variability of the misalignment, which may be less than 0.1 mrad, was not applied in this study.

To minimize the c.m. offset, the GRACE satellites perform c.m. calibration maneuvers regularly to locate the c.m. position. With this estimate, a c.m. trim mechanism adjusts the c.m. to be close to the proof mass by means of a moving mass. After this adjustment, the c.m. offset becomes very small. Because other simulation results showed that the  $f_{\text{c.m.}}$  can be negligible with smooth attitude motion,  $f_{\text{c.m.}}$  was not included in this paper.

One of the other errors,  $f_{\text{other}}$ , results from thruster firing, which might not be perfectly measured by the ACC due to its short duration. This error can be minimized by applying a proper ACC filtering and orbit integration method. Because this error is being investigated,  $f_{\text{other}}$  was not included in this paper.

Figure 4 compares the power spectrum of the individual ACC errors for a 450-km orbit altitude. The nongravitational acceleration is also plotted for comparison. The random noise is larger than the other errors. Both the attitude and misalignment errors affect the ACC measurement through interference from the other axis components. Therefore, their magnitudes are dependent on the magnitude of the ACC input, that is, nongravitational accelerations, such that

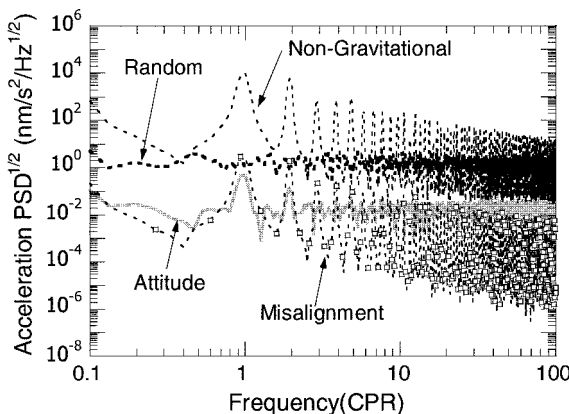


Fig. 4 Power spectrum of ACC errors at 450-km altitude.

these errors become more significant for lower-altitude orbits where larger atmospheric drag is present. The nongravitational acceleration at 300-km altitude (minimum mission altitude) is about one order of magnitude higher than the 450-km altitude acceleration. The corresponding attitude and misalignment errors are one order of magnitude higher as well.

### E. GPS Error Model

This study focused on the SST and ACC measurement errors because they are the major error sources affecting the gravity solution. For this reason, a relatively simple model was applied to the GPS measurements. The GPS tracking scenario assumed a constellation of 24 GPS satellites and 6 GPS ground stations. To analyze the effect of the number of stations, some experiments were performed by changing the number of stations from 6 to 24, but the gravity solution improvement was insignificant.<sup>13</sup> For this reason, the number of ground stations was limited to six. The GPS receivers were assumed to track all of the visible satellites. The elevation cutoff angles for the ground and flight receivers were 15 and 0 deg, respectively.

Gaussian random (white) noise with 5-mm standard deviation was applied for the single-phase-derived range measurements. The measurements were assumed to be corrected for ionosphere effects.

### F. Force Models

The EGM96 model,<sup>1</sup> which is a set of spherical harmonic coefficients, was used as the truth gravity field. A clone of EGM96, created by adding random numbers to the EGM96 coefficients, was used as the nominal gravity field. The difference between the clone and truth gravity coefficients represents the uncertainty level ( $1\sigma$ ) of the truth model. Other experiments showed that the gravity estimation accuracy is not sensitive to the choice of the gravity models. Various gravity models (e.g., different realizations of the clone models, JGM3, estimated gravity models from the first estimations, etc.) were tested for this purpose.

The Earth gravity field has both mean and time-varying gravity. The latter effect, including the tidal effect, can be compensated by use of an accurate nominal time-varying gravity model. Because the time-varying gravity study is being investigated, only mean gravity was considered in this paper.

For the truth nongravitational accelerations, atmospheric drag, solar, and Earth radiation pressure were applied. A simple atmospheric model that assumes a constant area in the direction of the relative wind was used, where the atmospheric drag was most dominant at the GRACE altitude (less than 500 km). The simulated ACC measurements were used for the nominal nongravitational accelerations.

## V. Simulation Results

### A. Computation Time and Solution Consistency

This estimation process is very complicated and computationally demanding. One simulation requires four orbit determination/simulation runs and two solver runs, as well as several other utility programs. One set of the simulation takes several days to complete with a CRAY SV1 supercomputer. This kind of complexity and computational time makes it difficult to apply comprehensive accuracy analysis, for example, Monte Carlo analysis. It can be shown that, within the linear region, the mean and covariance from a Monte Carlo simulation agree with the mean and covariance from a linear estimation approach. The number of estimation parameters [more than 15,000 for a  $(120 \times 120)$  gravity estimation] leads to questions related to parameter observability. If the information matrix is formed without any a priori information and if it can be inverted, the complete parameters set is observable, that is, it can be estimated. The observability of this problem is tied to the spatial distribution of the observations, and it has been demonstrated that an orbit arc length of 30 days provides global coverage and will yield a well-conditioned information matrix. The gravity covariance analysis results are included as part of the overall accuracy assessment.

Numerous simulations were performed with orbit and measurement models similar to the simulation described in this paper. Except for the accuracy difference due to the model differences, all of the results showed a similar level of accuracy. With the assumption that

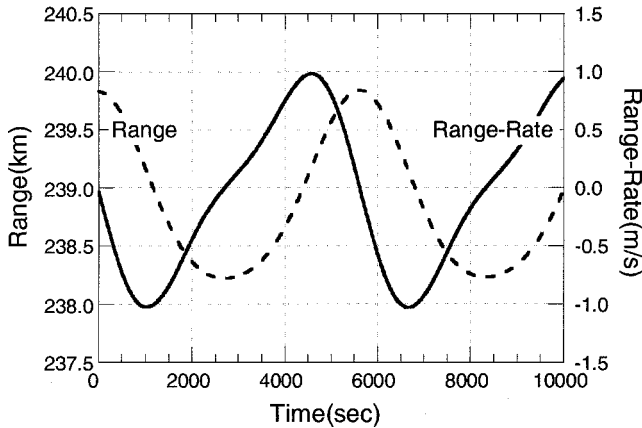


Fig. 5 Low-low intersatellite range and range-rate observables.

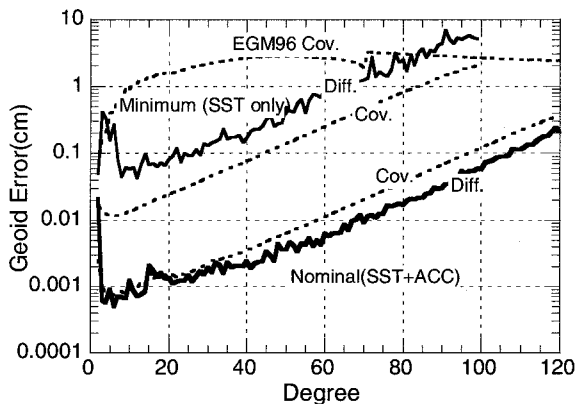


Fig. 6 Expected geoid height error from GRACE mission.

all of the significant error sources were applied in the simulations and an optimal estimation method was used, one can predict the estimated gravity accuracy from these simulation results.

#### B. SST Signal Characteristics

Figure 5 shows the time series of the typical range and range-rate signals. The amplitude of the range signal variation is about 1 km with a mean value of 239 km. The amplitude of the range-rate variation is about 1 m/s. Because the timescale is short, the secular effect, which dominates the long-term signal, is not shown in Fig. 5. One orbit period is around 5500 s and the 1 cycle per revolution (CPR) frequency is about  $1.8 \times 10^{-4}$  Hz.

The 1-CPR component, which is the dominant signal, is mainly due to the orbit eccentricity. The next dominant signal is the 2-CPR signal, which is due to the Earth's oblateness ( $J_2$ ). The high-frequency gravity signal is amplified in the range-rate observation due to the differentiation process. This amplification can be clarified in the spectral domain.

#### C. Expected Gravity Accuracy

The expected geoid height errors are presented in Fig. 6. The geoid represents a specific equipotential surface,<sup>1,15</sup> and this accuracy is directly related to the gravity field accuracy. The solid line labeled Diff. is computed from the difference between the truth and estimated gravity coefficients. The dotted line labeled Cov. is computed from the covariance matrix. The gravity coefficient errors are averaged for each degree, and the plot in Fig. 6 represents the overall error of the 14,000+ parameters. The differenced results show a good agreement with the covariance results. It shows up to 1000 times improvement over the current knowledge as represented by the EGM96 model.

A worst-case scenario was also performed, assuming the failure of the two ACCs. The nominal nongravitational accelerations predicted from a nominal force model replaced the ACC measurements, whereas the low-low SST measurement was still available.

This less-accurate nongravitational information degrades the gravity solution by two orders of magnitude, and the gravity improvement is confined to a very low 30 deg or less. However, it still shows some improvement over the current knowledge level. For a mission longer than 30 days, a more significant improvement would be obtained. The differenced results show a lower accuracy than the covariance results. Although the gravity accuracy from this simulation is limited to the specific orbit and measurement model conditions, one can expect that the accuracy from the actual mission goes between the nominal and worst cases.

#### D. Orbit Accuracy

The primary objective of this study is the analysis of the gravity accuracy, rather than the orbit accuracy. Most of the estimation algorithm developments are devoted to improve the gravity accuracy. In addition, the orbit accuracy is more sensitive to the simulation conditions than the gravity accuracy. For this reason, the details on the orbit accuracy results are not included in this paper. An orbit accuracy study, for instance, the observability analysis and development of an optimal estimation technique for the low-low SST, can be a future topic.

As with the gravity accuracy improvement, a significant improvement was observed for the orbit accuracy. This is because of the characteristics of the dynamic orbit determination method, which depends on the dynamic model accuracy. In addition, the high-precision ACC minimizes the nongravitational modeling error. This improvement demonstrates the importance of the gravity field accuracy in satellite orbit determination.

Although the orbit accuracies of other low-altitude satellites without ACCs are still limited by the nongravitational errors, we can expect that the accurate gravity field from the GRACE mission will improve the orbit accuracies of the previous satellites, for example, GEOSAT, ERS-1, etc., whose orbit errors mainly resulted from the large gravity errors.

## VI. Conclusions

Two major instrument models of the GRACE mission, the low-low intersatellite ranging and the ACC, along with their major error sources, were described. The ACC error is dominant in the low frequency, whereas the intersatellite range error is dominant in the high frequency. Therefore, the estimation of the long-wavelength gravity field is mainly limited by the ACC error, but the estimation of the short-wavelength field is limited by the intersatellite range error. To the extent that the error sources assumed in these simulations represent the actual error, the GRACE mission can achieve significant improvement in the study of the Earth's gravity field.

## References

- Dickey, J. O., Bentley, C. R., Bilham, R., Carton, J. A., Eanes, R. J., Herring, T. A., Kaula, W. M., Lagerloef, G. S. E., Rojstaczer, S., Smith, W. H. F., Van den Dool, H. M., Wahr, J. M., and Zuber, M. T., *Satellite Gravity and the Geosphere: Contributions to the Study of the Solid Earth and Its Fluid Envelope*, National Research Council, National Academy Press, Washington, DC, 1997, pp. 1-6, 29-33, 36.
- Davis, E. S., Dunn, C. E., Stanton, R. H., and Thomas, J. B., "The GRACE Mission: Meeting the Technical Challenges," International Astronautical Federation, Paper IAF-99-B.2.05, Oct. 1999.
- Wolff, M., "Direct Measurements of the Earth's Gravitational Potential Using a Satellite Pair," *Journal of Geophysical Research*, Vol. 74, No. 22, 1969, pp. 5295-5300.
- Mazanek, D. D., Kumar, R. R., Seywald, H., and Min, Q., "GRACE Mission Design: Impact of Uncertainties in Disturbance Environment and Satellite Force Models," American Astronautical Society, Paper AAS 00-163, Jan. 2000.
- Piscane, V. L., Ray, J. C., MacArthur, J. L., and Bergeson-Willis, S. E., "Description of the Dedicated Gravitational Satellite Mission (GRAVSAT)," *IEEE Transactions on Geoscience and Remote Sensing*, Vol. GE-20, No. 3, 1982, pp. 315-321.
- MacArthur, J. L., and Posner, A. S., "Satellite-to-Satellite Range-Rate Measurement," *IEEE Transactions on Geoscience and Remote Sensing*, Vol. GE-23, No. 4, 1985, pp. 517-523.
- Keating, T. P., Taylor, P., Kahn, W., and Lerch, F., "Geopotential Research Mission, Science, Engineering, and Program Summary," NASA TM-86240, 1986, pp. 69-73.

- <sup>8</sup>Wagner, C. A., "Improved Gravitational Recovery from a Geopotential Research Mission Satellite Pair Flying en Echelon," *Journal of Geophysical Research*, Vol. 92, No. B8, 1987, pp. 8147-8155.
- <sup>9</sup>Reigber, Ch., Schwintzer, P., Hartl, Ph., Ilk, K. H., Rummel, R., van Geldern, M., Schrama, E. J. O., Wakker, K. F., Ambrosius, B. A. C., and Leenman, H., "Study of a Satellite-to-Satellite Tracking Gravity Mission," European Space Research and Technology Centre, ESA Contract Rept. 6557/85/NL/pp(SC), Munich, March 1987, pp. 15-43.
- <sup>10</sup>Wakker, K. F., Ambrosius, B. A. C., and Leenman, H., "Satellite Orbit Determination and Gravity Field Recovery from Satellite-to-Satellite Tracking," Dept. of Aerospace Engineering, Delft Univ. of Technology, Rept. LR-605, Delft, The Netherlands, July 1989, pp. 220-228.
- <sup>11</sup>Mackenzie, R. A., and Moore, P., "A Geopotential Error Analysis for a Non Planar Satellite to Satellite Tracking Mission," *Journal of Geodesy*, Vol. 71, No. 5, 1997, pp. 262-272.
- <sup>12</sup>Sharma, J., "Precise Determination of the Geopotential with a Low-Low Satellite-to-Satellite Tracking Mission," Ph.D. Dissertation, Dept. of Aerospace Engineering and Engineering Mechanics, Univ. of Texas, Austin, TX, Dec. 1995.
- <sup>13</sup>Kim, J. R., "Simulation Study of a Low-Low Satellite-to-Satellite Tracking Mission," Ph.D. Dissertation, Dept. of Aerospace Engineering and Engineering Mechanics, Univ. of Texas, Austin, TX, May 2000.
- <sup>14</sup>Thomas, J. B., "An Analysis of Gravity-Field Estimation Based on Intersatellite Dual-I-Way Biased Ranging," Jet Propulsion Lab., California Inst. of Technology, JPL Publ. 98-15, Pasadena, CA, May 1999.
- <sup>15</sup>Leick, A., *GPS Satellite Surveying*, 2nd ed., Wiley, New York, 1995, pp. 247-271.
- <sup>16</sup>Kim, J. R., Key, K. W., and Tapley, B. D., "Simulation of High Accuracy Inter-Satellite Ranging Measurements," American Astronautical Society, Paper AAS 01-146, Feb. 2001.
- <sup>17</sup>Touboul, P., Bernard, A., Barlier, F., and Berger, C., "Air Drag Effect on Gradiometer Measurements," *Manuscripta Geodaetica*, Vol. 16, 1991, pp. 73-91.
- <sup>18</sup>Tapley, B. D., "Statistical Orbit Determination Theory," *Recent Advances in Dynamical Astronomy*, edited by B. D. Tapley and V. Szebehely, Reidel, Boston, 1973, pp. 396-425.
- <sup>19</sup>Yuan, D. N., "The Determination and Error Assessment of the Earth's Gravity Field Model," Ph.D. Dissertation, Dept. of Aerospace Engineering and Engineering Mechanics, Univ. of Texas, Austin, TX, May 1991.
- <sup>20</sup>Barlier, F., Berger, C., Falin, J. L., Kockarts, G., and Thuillier, G., "A Thermospheric Model Based on Satellite Drag Data," *Annals of Geophysics*, Vol. 34, No. 1, 1978, pp. 9-24.
- <sup>21</sup>Meditch, J. S., "Clock Error Models for Simulation and Estimation," Aerospace Corp., Aerospace Rept. TOR-0076 (6474-D1)-2, El Segundo, CA, July 1975.
- <sup>22</sup>Kosaka, M., "Evaluation Method of Polynomial Models' Prediction Performance for Random Clock Error," *Journal of Guidance, Control, and Dynamics*, Vol. 10, No. 6, 1987, pp. 523-527.
- <sup>23</sup>Stevens, H. D., Rodden, J., and Carrou, S., "Mass Expulsion Control for Precision Pointing Spacecraft," American Astronautical Society, Paper AAS 99-318, Aug. 1999.